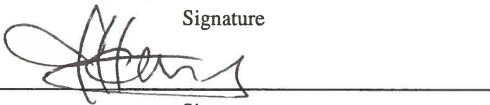


Gabrielle Farina

**1500 years of anchovy and sardine population response to coastal upwelling off Southern California**

submitted in partial fulfillment of the requirements for the degree of  
**Master of Science in Earth and Environmental Sciences**  
Department of Earth and Environmental Sciences  
The University of Michigan

  
Signature  
  
Signature  
Gabrielle Farina  
Department Chair Signature

Accepted by:  
MATT FRIEDMAN 30 JULY 2018  
Name Date  
INGRID HENDY 31 JULY 2018  
Name Date  
NADMI LEVIN 15 AUG 2018  
Name Date

I hereby grant the University of Michigan, its heirs and assigns, the non-exclusive right to reproduce and distribute single copies of my thesis, in whole or in part, in any format. I represent and warrant to the University of Michigan that the thesis is an original work, does not infringe or violate any rights of others, and that I make these grants as the sole owner of the rights to my thesis. I understand that I will not receive royalties for any reproduction of this thesis.

Permission granted.

Permission granted to copy after: \_\_\_\_\_

Permission declined.

  
Author Signature



# **1500 years of anchovy and sardine population response to coastal upwelling off Southern California**

5<sup>th</sup> Year Masters Thesis 2018

Gabrielle Farina

## **Abstract**

Young pelagic, planktivorous fish species feed on phytoplankton and zooplankton larvae, which respond to nutrient delivery by upwelling. Off the coast of Southern California, wind-driven coastal upwelling is affected by the position and strength of the North Pacific High Pressure system (NPH). When NPH strength increases, coastal upwelling intensifies and dry climate conditions prevail. Here we determine the abundance of four pelagic fish species; Northern anchovy (*Engraulis mordax*), Pacific sardine (*Sardinops sagax*), hake (*Merluccius productus*), and surfperch (Embiotocidae spp.), in Santa Barbara Basin (SBB) over the last 1500 years and relate population fluctuations to regional upwelling and the strength of the NPH. Proxies for marine productivity, drought and surface water masses based on sediment geochemistry are used to reconstruct NPH strength and surface ocean circulation. Sediment core SPR0901-02KC was collected from the SBB (34°16.8' N, 120°02.3' W) and sampled continuously at 0.5 cm resolution (~5-year resolution) for fish scale counts from which scale deposition rates (SDR) and relative abundance (%) were estimated. Anchovy scales generally comprise >50% of total scales. Anchovy SDRs were >30 scales cm<sup>-2</sup> year<sup>-1</sup> × 1000 between 510-675, 860-1075, 1425, 1500, 1560-1700 and 1750-1825, and 1870-1900 CE when the NPH was strong producing both intense coastal upwelling and drought in Southern California. Sardine SDRs (<20% of scales) were generally in phase with anchovy, with lower and more variable abundance. Sardine comprise >10% of scales between 680-875, 1050-1300, 1340-1380, 1480-1510 and 1690-1740 CE. Hake scales comprise ~30-50% of total scales and are most abundant between 760-1030 and 1275-1470 CE when Eastern Tropical North Pacific water entered the basin, with a maximum SDR of ~35 scales cm<sup>-2</sup> year<sup>-1</sup> × 1000. Surfperch scales generally comprise <10% of total scales. Anchovy abundance increases during intervals supporting a strengthening of the NPH, while hake respond to variations in poleward currents. Sardine and surfperch have no notable correlations with these environmental factors.

## Introduction

The abundance of lower-level consumers (animals that feed at or near the bottom of the food chain) in any marine food web depends largely upon the amount of nutrients available to photosynthetic organisms, as this determines regional primary productivity and therefore the amount of prey available to these consumers (Checkley et al., 2017; McClatchie et al., 2018). Primary productivity can vary greatly in response to environmental changes such as ocean circulation and nutrient availability (Anderson et al., 2008; Brzezinski and Washburn, 2011). Upwelling has a major control on nutrient availability as it brings nutrients into the photic zone for photosynthetic autotroph use (Rykaczewski and Checkley, 2008). Anchovy and sardine are examples of lower-level consumers as open-ocean fish species that feed mainly on zooplankton and phytoplankton (van der Lingen et al., 2009). As upwelling stimulates the growth of these planktonic populations through nutrient availability, anchovy and sardine populations off the western coasts of Chile, South Africa, and Southern California fluctuate in response to climate conditions that influence upwelling (Rykaczewski and Checkley, 2008; Contreras-Reyes et al., 2016; Schwartzlose et al., 1999). In the eastern Pacific, the populations of these two pelagic fish species have been observed to rise and fall in response to coupled oceanic-atmospheric systems, such as El Niño-Southern Oscillation (ENSO) and the Pacific Decadal Oscillation (PDO), that influence the North Pacific High atmospheric pressure system (NPH) and the Aleutian Low atmospheric pressure system (AL) (Cubillos and Arcos, 2002; Chavez et al., 2003; Skrivanek and Hendy, 2015). A recent 150-year reconstruction of anchovy and sardine populations in the Humboldt Current System off the western coast of South America found the two populations to dominate in alternating regimes largely driven by changes in upwelling conditions (Salvatteci et al., 2018).

Northern anchovy (*Engraulis mordax*) and Pacific sardine (*Sardinops sagax*) are small pelagic fish common in the eastern Pacific that are found off the coast of California (Soutar and Isaacs, 1974). Anchovy inhabit the region year-round but migrate to deeper offshore waters in winter and back to shallow onshore waters in spring (Kucas Jr. et al., 1986). Sardine, on the other hand, migrate between the coasts of the Pacific Northwest and Southern California and are mainly found in Southern California at the height of their spawning season from late winter to early spring (Checkley et al., 2017; Demer et al., 2012 and references therein). As primary consumers, their response to fluctuations in phytoplankton and algae abundance is much more

rapid and dramatic than that of larger, higher level consumers such as larger fish, sea birds, dolphins, and sea lions (McClatchie et al., 2017 and references therein; McClatchie et al., 2018 and references therein). Though both sardine and anchovy are planktivores, they feed on different sized planktonic prey and are therefore not in direct competition with one another for food resources (Rykaczewski and Checkley, 2008). Anchovy possess coarse gill rakers that allow them to capture relatively large phytoplankton and zooplankton, mainly large diatom and copepod species (van der Lingen et al., 2009). Sardine have finer gill rakers and as a result can capture prey as small as  $<10\mu\text{m}$ , notably dinoflagellates, smaller diatom and copepod species, and euphausiids (van der Lingen et al., 2009). These anatomical differences have been hypothesized to allow each species to thrive under different environmental conditions (Rykaczewski and Checkley, 2008). Anchovy's larger gill rakers make them best equipped to feed in regions of intense coastal upwelling where large nutrient influxes fuel rapid growth of large plankton very locally, while sardine's smaller gill rakers are thought to be most effective in regions of broad offshore upwelling caused by wind-stress curl where primary productivity by smaller plankton is generally higher over large regions (Rykaczewski and Checkley, 2008). Additionally, ideal sea surface temperatures differ between the two species, as anchovies spawn in SSTs between 12-16°C while sardine spawn in warmer water in the 14-16°C range (Checkley et al., 2000; Demer et al., 2012 and references therein).

Hake (*Merluccius productus*) and surfperch (Embiotocidae spp.) are two more pelagic fish species that may also be associated with coastal upwelling in Southern California. Hake feed mainly on euphausiids, shrimp, and small fish such as anchovy, herring, and sand lance (Alverson and Larkins, 1969; Demer et al., 2012; Patterson et al., 2002). Increases in hake abundance have been associated with a strong California Undercurrent (CU), as the poleward flow decreases the amount of energy required by individual fish to migrate northward (Agostini et al., 2006). Surfperch diet consists primarily of crustaceans such as amphipods and shrimp larvae (Patterson et al., 2002). Anchovy, sardine, hake, and surfperch are all deciduous fish that shed their scales annually as a defense against predators (Field et al., 2009). As a result, scales from these species are commonly deposited on the seafloor and subsequently preserved in the sedimentary record (Baumgartner et al., 1992; Soutar and Isaacs, 1974).

Sediment from the Santa Barbara Basin (SBB) off the coast of Southern California has been employed in numerous paleoclimate reconstructions (Hendy et al., 2013 and references

therein). Sediments in this basin are anoxic as bottom waters sit within the Oxygen Minimum Zone, and local high biological productivity results in a high oxidant demand (Wang et al., in prep). The biogenic sediments are very well-preserved, as the absence of oxygen in SBB bottom waters prevents the decomposition of deposited biogenic material such as fish scales (Baumgartner et al., 1992; Soutar and Isaacs, 1974). The anoxic bottom waters also prevent benthic macrofauna from disturbing sediments after they are deposited. This preservation of SBB sediment allows for the clear observation of high-resolution varves. Varves are annually deposited couplets of biogenic and lithogenic layers of sediment, or laminae (Baumgartner et al., 1992; Hendy et al., 2015). Biogenic laminae are generally deposited in spring and summer, while lithogenic laminae are generally deposited in autumn and winter (Hendy et al., 2015). An unusually strong NPH can cause drought in Southern California, reducing the amount of sediment rivers deposit in the basin as decreased precipitation leads to less river runoff during this time (Hendy et al., 2015). Alternatively, an unusually weak NPH can lead to extreme rainfall in winter months, causing more river runoff and more therefore more sediment deposition than usual (Hendy et al., 2015; McClatchie et al., 2017). In this way, the geochemistry of the basin sediments can record droughts and floods providing a record of NPH strength. An independent measure of NPH strength is important because a strong NPH also causes strong coastal upwelling in the summer, as its northerly migration intensifies the equatorward winds that are responsible for coastal upwelling (Schroeder et al., 2013). This brings cold, nutrient-rich water to the surface and increases biological productivity, which impacts forage fish populations (Anderson et al., 2008; Brzezinski and Washburn, 2011; Rykaczewski and Checkley, 2008).

One of the primary aims of previous anchovy and sardine studies in this region has been to identify the influence of climatic variations on the abundance of the two species. While the question of whether anchovy and sardine populations fluctuate “in phase” or “anti-phase” has been central to several studies, the conclusions drawn are conflicting (Baumgartner et al., 1992; Chavez et al., 2003; Field et al., 2009; Finney et al., 2010; McClatchie et al., 2017; Salvatteci et al., 2018). Early studies of SBB sediment cores and the relationship between anchovy and sardine using scale deposition rates observed that the populations were moderately in phase over timescales of several hundred years (Baumgartner et al., 1992; Soutar and Isaacs, 1974). The populations of both species were found to collapse in natural cycles, with recovery intervals that varied between 30 and 100 years (Baumgartner et al., 1992). However, a subsequent study

comparing modern sardine and anchovy landings with records of atmospheric-oceanic data, such as atmospheric CO<sub>2</sub>, global air temperature, SST and PDO, concluded that anchovy and sardine populations fluctuate out of phase with each other (Chavez et al., 2003). This study determined that anchovy and sardine dominate the pelagic fish population off the West Coast of North America in “regimes” that correspond to opposing atmospheric and oceanic conditions, associated with decadal to interannual climate variability (e.g. the PDO and ENSO) (Chavez et al., 2003). The anchovy regime was associated with cold sea surface temperatures (SSTs), strong coastal upwelling, strong California Current (CC), and a shallow thermocline in the eastern North Pacific (Chavez et al., 2003). The sardine regime was associated with warm SSTs, weak coastal upwelling, weak CC, and a deep thermocline in this region (Chavez et al., 2003).

The presence of anchovy and sardine regimes was disputed, however, by several studies that found positive correlations between anchovy and sardine populations on multidecadal timescales in SBB (Baumgartner et al., 1992; Field et al., 2009; Finney et al., 2010; McClatchie et al., 2017; Soutar and Isaacs, 1974). A study that compared stock-recruit and temperature-recruit relationships for Pacific sardine to environmental parameters in Southern California observed sardine to be negatively correlated with warm SSTs, directly contradicting the idea that sardine abundance increases with SST (Chavez et al., 2003; McClatchie et al., 2010). From 1991-2008, SSTs were anomalously warm in all but one year, while all but three years over the same time interval had negative sardine recruitment anomalies (McClatchie et al., 2010). Furthermore, in a study of the influence of the PDO on sardine biomass in Southern California, sardine abundance was observed to be unrelated to this multidecadal ocean-atmosphere system (McClatchie, 2012). Thus, it is possible that sardine populations are driven by interannual (<10-year) environmental changes such as ENSO and the impact of commercial fishing on sardine biomass rather than fluctuations in decadal and multidecadal ocean-atmosphere systems such as the PDO (McClatchie, 2012; Chavez and Chavez-Hidalgo, 2013).

An understanding of how these fish populations fluctuate over time is crucial to understanding how higher trophic level organisms in the California Current ecosystem respond to climate change. Anchovy and sardine are a major food source for several predators, including sea lions, dolphins, humpback whales, and sea birds (Checkley et al., 2017; McClatchie et al., 2017; McClatchie et al., 2018; Patterson et al., 2002). Both anchovy and sardine catches in Southern California have been low in recent years; the anchovy fishery is open but restricted, and

the sardine fishery has been closed since 2015 (McClatchie et al., 2018). These limitations on commercial fishing have allowed for the recent recovery of the California sea lion, but the prey needs of this marine mammal far exceed the commercial catch of these forage fish, and future climate change may have a significant impact on the California sea lion (McClatchie et al., 2018).

Here we reconstruct 1,500 years of anchovy, sardine, hake, and surfperch populations in the SBB, CA to further investigate the relationship between anchovy and sardine abundance as well the response of all four species to changing environmental parameters influenced by climate variability. A more thorough understanding of these species' responses to coastal upwelling and surface water circulation will contribute to determining the sustainable commercial harvest of these important forage fish, reducing ongoing uncertainty in the industry (McClatchie et al., 2017).

## Methods

### *Data collection*

SPR0901-02KC (588 m water depth; 34°16.8.450 N, 120°02.3320 W) and SPR0901-06KC (591 m water depth; 34°16.914 N, 120°02.419 W) were collected from the SBB in 2009 using a 17×17 cm Kasten corer (Figure 1). SPR0901-02KC was continuously sampled 0.5 cm intervals (~5-year resolution) while SPR0901-06KC was continuously sampled at 1 cm intervals. Samples were washed using deionized water over a 125 µm sieve with the coarse fraction air dried in an oven and stored in glass vials. Beginning in January 2017, samples were separated with a 425 µm sieve, and sediment >425 µm was observed under a binocular dissecting microscope. Anchovy, sardine, hake, and surfperch scales were identified in each sample (Figure 2). A small paintbrush was wet with deionized water and used to remove scales from the microscope tray and place them on a separate cardboard assemblage slide labeled with core name, sample depth, and fish species. Once on new slides, the number of whole scales and scale fragments for each species was counted and recorded.

### *Scale Identification*

Species of fish scales were identified using descriptions and photographs from Patterson et al., 2002. Identifications were made based on size, shape, and the patterns of radii and circuli. Radii are defined as grooves that extend outward toward the scale margins from the focus; they

either begin at the focus (primary radii) or between the focus and the margin (secondary radii) (Patterson et al., 2002). Circuli are elevated lines that generally follow the outline of the scale (Patterson et al., 2002). The focus is the point of origin of scale growth, often located near the center of the scale (Patterson et al., 2002).

Thickness and durability of scales can be an additional identifying factor (Patterson et al., 2002). Anchovy scales are highly flexible and vulnerable to erosion and subsequent fracturing (Patterson et al., 2002). The anterior field of this scale type is tri-lobed, and the overall scale is generally circular in shape and somewhat large. The location of the focus is variable and can be unclear, but is defined as the location of the first concentric circuli (Patterson et al., 2002). Circuli and fractures are usually transverse to one another (Patterson et al., 2002). Sardine scales are generally the largest of the four scale types observed in this study. Their relative durability makes them more likely to be found intact than less durable anchovy or surfperch scales (Patterson et al., 2002). The shape of sardine scales ranges from ovate to rectangular, with larger scales being more rectangular. The location of the focus is near and slightly above the posterior field, and both the circuli and the fractures follow the general scale outline (Patterson et al., 2002). Fractures resemble radii, but radii themselves are not present on sardine scales (Patterson et al., 2002). Hake scales are usually an oval shape and are smaller than both anchovy and sardine scales. The focus is close to the scale center, and circuli follow the outline of the scale. Although hake scales are generally considered to be brittle and tend to break along circuli (Patterson et al., 2002), these scales were more frequently found intact than any other species in the samples. Surfperch scales are rectangular in shape with a posterior field that is rounded in shape (Patterson et al., 2002). Circuli follow the outline of the scale and are usually continuous. The focus is generally close to the edge of the posterior field, and the scalloped edge of the anterior field makes this scale type distinguishable from others (Patterson et al., 2002).

### *Age Model*

An age model using radiocarbon dating as well as counting sedimentary microlayers (varves) was used in order to assign calendar ages to fish scales from sediment cores SPR0901-02KC and SPR0901-06KC (Hendy et al., 2013; Du et al., 2018). Approximately 40  $^{14}\text{C}$  ages from planktonic foraminiferal carbonate in SPR0901-06KC ( $34^{\circ}16.914\text{ N}$ ,  $120^{\circ}2.419\text{ W}$ ) were used to generate an age model (Hendy et al., 2013). A variable reservoir age was applied to the

<sup>14</sup>C dates (Hendy et al., 2013; Du et al., 2018). The most recent ~300 years of the core were determined by counting varves (Schimmelmann et al., 1992; Hendy et al., 2013) including the core top (1905 CE), gray layers (1861-62 and 1761 CE), a Macoma layer (1841 CE), and a turbidite (1811 CE) (Du et al., 2018). The thicknesses of sedimentary layers created by instantaneous events such as flood layers and turbidities were removed from the original sample depths (Table 1) (Du et al., 2018). The software BACON 2.2 was then used to convert these radiocarbon dates and instantaneous deposition dates into sediment deposition histories using Bayesian statistics (Blaauw and Christen, 2011). This age model was transferred between cores using known turbidites and flood layers as well as 12 visually distinct additional marker horizons determined by distinguishable differences in core fabric such as varve color and thickness (Du et al., 2018).

#### *Scale Deposition Rates*

The scale deposition rate for each 0.5 cm of the core was calculated using the following formula.

$$\text{Scale deposition rate (scales} \times 1000 \text{ cm}^{-2} \text{ year}^{-1}) = \text{Linear sedimentation rate (cm year}^{-1}) \times \\ \text{fish scale count (scales cm}^{-3}) \times 1000$$

#### *Pearson Correlations*

For statistical analysis, scale deposition rates, relative abundance, and the ratio of total sardine scales to total anchovy scales were resampled at 5-year intervals using the program Analyseries 2.0.8. To analyze the relationships between these fish populations and their environment, Pearson correlations between fish scale data and several geochemical datasets were calculated using Microsoft Excel. Bulk sediment  $\delta^{15}\text{N}$  (Wang et al., in prep) was used as a proxy for the presence of denitrified water. Scanning XRF derived Br/Cl was used as a proxy for total carbon export, while Ca/Ti and Si/Ti from Hendy et al., 2015 and Wang et al., in prep were used as proxies for biogenic  $\text{CaCO}_3$  and biogenic  $\text{SiO}_2$  production, respectively. Ti was used as a proxy for precipitation-driven river runoff in Southern California (Du et al., in prep; Napier and Hendy, 2018). Pearson correlations were undertaken on years 510-1910 CE, and n = 281. Geochemical data were produced from sediment in Kasten core SPR0901-03KC (Hendy et al., 2015; Wang et al., in prep; Du et al., in prep).

To estimate the error in scale abundance, fish scale counts from SPR0901-02KC were compared to counts from SPR0901-06KC for 3 intervals (775-810, 945-1065, and 1695-1915 CE) spanning the last 1,500 years. Both cores were resampled at 5-year intervals using the program Analyseries 2.0.8. The average and standard deviation of SDR of both cores was then calculated for each species to provide an estimate of counting error.

## Results

### *Scale Deposition Rates*

Figure 3 shows calculated scale deposition rates (in scales  $\times$  1000 cm $^{-2}$  year $^{-1}$ ) for whole and total scales of anchovy, sardine, hake, and surfperch for ~470-1910 CE. Anchovy SDRs are generally the highest of all four species, with maximums of ~100 total scales  $\times$  1000 cm $^{-2}$  year $^{-1}$  at approximately 650 and ~65 total scales  $\times$  1000 cm $^{-2}$  year $^{-1}$  at approximately 875 and again at approximately 1575 CE. Whole scale SDR peaks at approximately 10 whole scales  $\times$  1000 cm $^{-2}$  year $^{-1}$  around 670 CE. Anchovy SDRs are highest between 500 and ~1200 CE. Periods when anchovy SDRs were >30 total scales  $\times$  1000 cm $^{-2}$  year $^{-1}$  occur between 510-675, 860-1075, 1425, 1500, 1560-1700 and 1750-1825, and 1870-1900 CE. Sardine SDRs are much lower than anchovy and exhibit greater variability. Sardine total scale SDR reaches a maximum of ~20 total scales  $\times$  1000 cm $^{-2}$  year $^{-1}$  at 1050, 1500, and 1725 CE, while the maximum whole scale SDR counts of 12 scales  $\times$  1000 cm $^{-2}$  year $^{-1}$  occur at ~1875 CE. The highest sardine SDRs mostly occur between ~1050-1500 CE. Though they do not exhibit fluctuations of similar magnitude, anchovy and sardine SDRs generally vary in phase with one another. Hake SDRs are often higher than sardine SDRs but less than anchovy SDRs. Unlike the other three species, hake SDRs are generally higher for whole scales than for scale fragments. Hake total SDRs reach maximum values of ~35 total scales  $\times$  1000 cm $^{-2}$  year $^{-1}$  at 1025 and ~30 total scales  $\times$  1000 cm $^{-2}$  year $^{-1}$  at 1450 CE. Maximum hake whole SDRs occur at ~28 total scales  $\times$  1000 cm $^{-2}$  year $^{-1}$  at 1450 CE. The highest hake SDRs occur between ~900 and 1475 CE. Surfperch SDRs are generally the lowest of the four species, with maximum rates at ~14 total scales  $\times$  1000 cm $^{-2}$  year $^{-1}$  (~7 whole scales  $\times$  1000 cm $^{-2}$  year $^{-1}$ ) at 1600 CE. Surfperch scales are highest between ~1550-1825 CE.

### *Sardine-Anchovy Ratio*

The ratio of total sardine to anchovy scales (Figure 4A) is generally very low (0.0-0.2) between ~510-1250 CE, with the exception of a peak of ~0.4 at ~800 CE. Between 1250-1850,

the ratio is generally higher (~0.3-0.4) reaching a maximum ratio of ~0.55 at ~1500 CE, and 1.0 at ~1775 CE. The data for the ratio of whole sardine to anchovy scales is less complete due to the frequent absence of samples containing whole scales. This ratio is highest between 650-875 and 1050-1300 CE, with several peaks of ~0.3-0.5 during these intervals and two peaks of 1.0 at ~825 and ~1500 CE.

### *Relative Abundance*

Relative abundance of fish scales is shown in Figure 4B. Anchovy is the most abundant of the four species, dominating relative abundance (%) from ~510-1200 CE when the species often accounts for >50% of the scales present. After ~1200 CE, anchovy relative abundance often decreases below 50% but rarely falls to <30% of the scales. Sardine scales are much less abundant than anchovy, comprising >10% of the scales between 680-875, 1050-1300, 1340-1380, 1480-1510 and 1690-1740 CE. Hake scale relative abundance is generally greater than sardine, generally comprising ~30-50% of the scales and with the highest relative abundance (~50-70%) between 1210-1500 and 725-1075 CE. Surfperch are a minor contributor to scales deposited (<20%) with the exception of 700, 1100, 1225, 1500-1650, 1690-1725 CE when they comprise ~20-70% of the relative scales present.

### *Pearson Correlations*

Table 2 shows Pearson correlation coefficients for the relationships between fish species absolute and relative scale abundance. Anchovy SDRs are moderately positively correlated with sardine and hake SDRs and not correlated with surfperch SDR. As expected, each species' SDR shows moderate to strong positive correlations with its own relative abundance. Anchovy SDRs have moderate negative correlations with sardine, hake, and surfperch relative abundance as well as with sardine/anchovy ratio. The sardine/anchovy ratios correlate positively with sardine SDR, surfperch SDR, and surfperch relative abundance while negatively correlating with hake SDR.

Table 3 shows Pearson correlation coefficients for fish scale data (SDR, %, and sardine/anchovy ratio) with geochemical proxies for environmental factors ( $\delta^{15}\text{N}$ , Br/Cl, Ca/Ti, Ti, and Si/Ti). All correlations between fish scale data and geochemical data are moderate in strength (0.200 to 0.300 or -0.200 to -0.300). Titanium correlates negatively with anchovy and hake SDR. Br/Cl correlates negatively with anchovy and hake SDR, and positively with sardine

relative abundance and sardine/anchovy ratio. Ca/Ti is positively correlated with anchovy SDR, and  $\delta^{15}\text{N}$  correlates positively with hake SDR. Si/Ti shows no correlation with any fish scale data. All geochemical proxies are shown in Figure 5.

#### *Fish Scale SDR Average and Error*

The average of fish scale SDRs between cores SPR0901-02KC and SPR0901-06KC is displayed in Figures 6 and 7. Scale count error is the standard deviation of the average SDR between the two cores. As expected, scale fragment counts tend to have more error than whole scale counts for all species with the exception of hake. Average anchovy total scale count generally ranges from  $20\pm10$  to  $30\pm20$  scales  $\text{cm}^{-2} \text{ year}^{-1} \times 1000$ . Average sardine total scale count is usually between  $2\pm1$  and  $10\pm8$  scales  $\text{cm}^{-2} \text{ year}^{-1} \times 1000$ . Average hake total scale count normally ranges from  $6\pm3$  to  $20\pm12$  scales  $\text{cm}^{-2} \text{ year}^{-1} \times 1000$ . Average surfperch total scale count is generally between  $2\pm1$  and  $5\pm5$  scales  $\text{cm}^{-2} \text{ year}^{-1} \times 1000$ . Anchovy error is highest at 975, 995, 1000, 1745, and 1750 CE. Sardine error is highest at 1045-1055, 1720, 1725, and 1875 CE. Hake error is highest at 1680 and 1745-1755 CE, and surfperch error is highest at 1690-1730, 1790-1800, 1890, and 1895 CE.

## **Discussion**

### *Relationships between pelagic fish species*

Anchovy and sardine have previously been thought to prefer opposing environmental conditions and therefore fluctuate anti-phase to one another, with anchovy dominating during periods of strong coastal upwelling, a strong CC, and cold water, and sardine dominating during periods of weak coastal upwelling, a weak CC, and warm water (Chavez et al., 2003; Salvatteci et al., 2018). However, anchovy and sardine scale deposition rates from SPR0901-02KC vary in phase with one another, suggesting that the populations of both species fluctuate together rather than oppositely. Observations of alternating anchovy and sardine regimes are based on a relatively short time observational records (<100 years), and these regimes are now hypothesized to be unique to the late twentieth century in SBB as well as Peru and Japan (Valdés et al., 2008; MacCall et al., 2009; Kuwae et al., 2017 and references therein). Furthermore, it has been suggested that the two species naturally fluctuate in phase on timescales spanning several centuries, and that their out-of-phase fluctuations over the last century might be the result of

commercial fishing (Field et al., 2009; Finney et al., 2010; McClatchie et al., 2017; Rykaczewski and Checkley, 2008). As this study spans from 510-1910 CE, our results support this proposed explanation. Error in absolute scale deposition is relatively high between cores SPR0901-06KC and SPR0901-02KC, but the general patterns of anchovy and sardine population fluctuation are similar. The inconsistency of absolute SDR between these cores is likely a result of the low number of scales found in core samples, which have limited spatial coverage.

Moderately strong positive Pearson correlations (Table 2) between anchovy, sardine, and hake SDR in SBB sediments show that the absolute population abundance of these three species tends to in phase with one another. This directly contradicts the anti-phase hypothesis presented by Chavez et al. (2003) and supports the in-phase hypothesis presented later on (Field et al., 2009; Finney et al., 2010; McClatchie et al., 2017). However, negative correlations between sardine relative abundance (%) and both anchovy and hake SDRs imply that relative abundance of sardine increases when overall fish abundance is low. Although surfperch SDRs show no correlation with other SDRs, the positive correlation of sardine/anchovy ratio with both surfperch SDR and surfperch relative abundance indicates that sardine and surfperch may potentially be most abundant in similar conditions. As with sardine relative abundance, negative correlations between surfperch relative abundance and anchovy and hake SDRs suggests that when surfperch relative abundance is high, it is likely at a time when overall fish abundance is low. Little is known about the environmental conditions driving surfperch population fluctuations, however.

Within the 1,500-year record, there are some brief intervals during which the anchovy SDR is high while the sardine SDR is low, including 510-620, 860-1000, and 1500-1650 CE. These inconsistencies with the general trend may be a result of unusually low water temperatures, as sardine prefer water that is 14-16°C while anchovy live in water between 12-16°C (Checkley et al., 2000; Demer et al., 2012). Though some research has indeed found SST to be somewhat cool from 860-1000 and 1500-1650 CE, other findings indicate no substantial decrease in SST in this region during the Little Ice Age (1500-1840 CE) (McCabe-Glynn et al., 2013; Zhao et al., 2015). These short intervals are reminiscent of the “anchovy regimes” characterized by cold water and strong upwelling that were observed by other studies (Chavez et al., 2003; Valdés et al., 2008; Salvatteci et al., 2018).

### *Pelagic fish and regional environmental changes*

Titanium is a component of continental lithogenic sediment that is delivered to SBB by river runoff (Hendy et al., 2015). Measurements of Ti concentrations in core SPR0901-03KC in SBB can therefore be used to determine the relative amounts of terrestrial sediment deposited by river runoff over time (Hendy et al., 2015). As river runoff is heavily influenced by the quantity of regional rainfall, the amount of terrestrial sediment runoff (and therefore the amount of Ti present) may be used to infer a regional rainfall record (Hendy et al., 2015; Heusser et al., 2015) with high Ti concentrations indicating frequent rainfall and low concentrations associated with drought conditions. As drought and coastal upwelling in this region both result from a strong NPH, we predict that the presence of drought should be coincident with coastal upwelling conditions in SBB (Hendy et al., 2015; Heusser et al., 2015). This prediction is supported by correlations of lithogenic input from river runoff and drought-adapted vegetation proxies, with silicoflagellate and diatom species that prefer upwelling conditions (Barron et al., 2015; Heusser et al., 2015). The negative correlation of Ti with both anchovy and hake SDRs indicates these species are more abundant when river runoff in Southern California is low during drought conditions (Hendy et al., 2015; Heusser et al., 2015). This result was anticipated because anchovy and hake are known to be more abundant during periods of increased biological productivity (Agostini et al., 2006; Chavez et al., 2003; Salvatteci et al., 2018) supported by intervals of coastal upwelling at 850-900, 1100-1125, 1275-1325, 1400-1500, and 1725-1775 CE. The lack of a negative correlation between sardine SDR and Ti concurs with previous conclusions that sardine abundance is not particularly high in coastal upwelling conditions (Chavez et al., 2003; Salvatteci et al., 2018). On the other hand, the lack of a *positive* correlation as well disagrees with these authors' suggestions that sardine fare poorly when coastal upwelling occurs. Instead, these data suggest that sardine are responding to environmental conditions unrelated to coastal upwelling strength.

Though most literature only associates pelagic fish populations with coastal upwelling or simply “upwelling,” these species may actually be influenced by two distinct types of upwelling: coastal upwelling and wind-curl upwelling (Chavez et al., 2003; Checkley et al., 2009; Field et al., 2009; Finney et al., 2010; Salvatteci et al., 2018; Valdés et al., 2008; Wang et al., in prep.). Coastal upwelling is caused by the northward migration of the NPH in summer months, which strengthens equatorward winds along the California Coast that cause intense localized upwelling

close to shore (Schroeder et al., 2013; Wang et al., in prep). Wind-stress curl is described as a horizontal shear in wind stress, which changes the direction of Ekman transport and subsequently causes vertical transport of water, or wind-stress curl upwelling (Rykaczewski and Checkley, 2008; Wang et al., in prep). This type of upwelling generally occurs at much lower velocities and over a significantly larger area of the California Current System (CCS) than coastal upwelling, as it can occur up to 200 km offshore, as opposed to the 5-30 km offshore range of coastal upwelling (Wang et al., in prep). As a result, both of these upwelling types are important nutrient delivery processes (Rykaczewski and Checkley, 2008; Wang et al., in prep). Sardine have been hypothesized to be more closely associated with wind-stress curl upwelling, as the slower velocities tend to aid in the biological productivity of the relatively small plankton (down to 10  $\mu\text{m}$ ) such as the dinoflagellates and small diatom and copepod species that are sardine's main food source (Rykaczewski and Checkley, 2008). The possible dependence of sardine on wind-stress curl upwelling rather than coastal upwelling could explain why no correlation was found between sardine and drought in this study, as wind curl upwelling does not require the NPH to be as intense and stationary (Wang et al., in prep).

$\text{Br}/\text{Cl}$  has stronger correlations with the fish scale data than does  $\text{Ti}$ ,  $\text{Ca}/\text{Ti}$ ,  $\text{Si}/\text{Ti}$ , or  $\delta^{15}\text{N}$ . As  $\text{Br}$  is present in both biogenic material and in seawater, it is normalized to  $\text{Cl}$ , which is present in seawater but not biogenic material (Hendy et al., 2015). This normalization eliminates the seawater component of the  $\text{Br}$  measurement and isolates the biogenic  $\text{Br}$  component (Hendy et al., 2015). In this study,  $\text{Br}/\text{Cl}$  is used as a proxy for total carbon export, or the amount of organic carbon from the water column that becomes buried and preserved in the sedimentary record.  $\text{Br}/\text{Cl}$  is negatively correlated with anchovy and hake SDRs, indicating that these two species are more abundant at times when carbon burial in SBB sediments is reduced. If carbon export is the direct result of coastal upwelling, then these results are inconsistent with the hypotheses that anchovy fare well in coastal upwelling conditions (Chavez et al., 2003; Salvatteci et al., 2018). The nutrients delivered by coastal upwelling are thought to promote biological productivity, which in turn increases total carbon production as large populations of phytoplankton and zooplankton are subsequently available for burial in seafloor sediment (Rykaczewski and Checkley 2008; Wang et al., in prep). However, carbon export is not just related to production, but also influenced by the delivery of organic matter to the seafloor and the preservation of organic carbon which may have been decreased by anaerobic decomposition or

increased by instantaneous depositional events in SBB (Wang et al., in prep). Br/Cl is positively correlated with the relative abundance of sardine (% and sardine/anchovy ratio), indicating that sardine tend to dominate over other species during periods of increased carbon export. This is also inconsistent with the findings that “sardine regimes” are characterized by lower productivity (and therefore lower carbon export, as this is thought to be consistent with total organic carbon in the water column) (Chavez et al., 2003; Salvatteci et al., 2018; Wang et al., in prep). In a 250-year core taken from the Mejillones Bay in northern Chile, a similar positive correlation was found between both sardine and anchovy SDR and organic carbon flux (a proxy for biological productivity); however, this relationship was based absolute fish abundance rather than relative fish abundance as in SBB (Valdés et al., 2008).

$\delta^{15}\text{N}$  is used here as a proxy for the presence of denitrified water, as lighter  $\delta^{14}\text{N}$  is preferentially taken up during denitrification while heavier  $\delta^{15}\text{N}$  is left behind (Wang et al., in prep) No correlation between either anchovy or sardine SDRs and  $\delta^{15}\text{N}$  was found in SBB in core SPR0901-02KC. This result is similar to Mejillones Bay, but the absence of a correlation in this case is attributed to the higher oxygen levels in the Bay, which are assumed to be associated with lower  $\delta^{15}\text{N}$  levels in the water column (Valdés et al., 2008). A positive correlation exists between  $\delta^{15}\text{N}$  and hake SDR, indicating that hake abundance tends to be high in the presence of denitrified water.  $\delta^{15}\text{N}$  is also negatively correlated with surfperch relative abundance, implying that surfperch are less abundant when denitrified water enters SBB. For  $\delta^{15}\text{N}$  to be present in SBB sediments, denitrified water needs to be reintroduced to the photic zone in order to be taken up by primary producers and subsequently deposited in seafloor sediment when these primary producers die (Wang et al., in prep). The denitrified water is likely sourced in the Eastern Tropical Pacific and transported northward by the California Undercurrent (CU) to SBB (Wang et al., in prep). For the denitrified water to rise up through the water column, both a strong poleward flow and coastal upwelling must occur (Want et al., 2017). From this we can infer that hake abundance increases and surfperch relative abundance decreases in the combined presence of both strong poleward flow and coastal upwelling. This supports previous findings that hake abundance increases during years with a strong CU, as the poleward flow positions them closer to food sources and aids in their northward migration (Agostini et al., 2006).

In this study scanning XRF Ca/Ti is used as a proxy for biogenic  $\text{CaCO}_3$  production. Ca is found in biogenic  $\text{CaCO}_3$  produced mainly by coccolithophorids and foraminifera, but it is

also found in terrestrial sediments (Wang et al., in prep). As Ti is only found in terrestrial sediments, normalization of Ca to Ti eliminates terrestrial Ca and isolates the biogenic Ca component (Hendy et al., 2015). A positive correlation between Ca/ Ti and anchovy SDR indicates that anchovy abundance is high at times of coccolithophorids and foraminifera productivity. However, this correlation contradicts the widely accepted hypothesis that anchovy thrive in upwelling conditions, as diatoms ( $\text{SiO}_2$ -based phytoplankton) are considered to be the primary producers most associated with coastal upwelling in SBB (Anderson et al., 2008; Chavez et al., 2003; McClatchie et al., 2017; Salvatteci et al., 2018; Venrick, 1998). Furthermore, coccolithophorids have been found to dominate phytoplankton populations only during non-upwelling conditions in Portugal (Abrantes and Moita, 1997). However, some coccolithophorids have also been found to be present during SBB coastal upwelling, so the correlation between Ca/Ti and anchovy SDR does not entirely contradict previous findings (Venrick, 1998). The absence of correlations between Ca/Ti and sardine, hake, and surfperch SDRs imply that these fish species may not be strongly influenced by the abundance of carbonate-based primary producers.

Similar to Ca, Si is found in both terrestrial sediments and in biogenic material ( $\text{SiO}_2$  produced by phytoplankton and zooplankton, mainly diatoms and silicoflagellates), so normalization to Ti isolates the biogenic component and eliminates the terrestrial component (Hendy et al., 2015; Wang et al., in prep). The lack of correlation between Si/Ti and fish scale data is unexpected, as diatoms have been found to be a primary phytoplankton associated with coastal upwelling in SBB as well as a similar upwelling system in Portugal (Abrantes and Moita, 1997; Anderson et al., 2008; Barron et al., 2015; Venrick, 1998). It is possible that the Si/Ti data may not accurately represent the amount of biogenic  $\text{SiO}_2$  in the water column at the time that it was deposited on the seafloor. Additionally, dissolution of  $\text{CaCO}_3$  and  $\text{SiO}_2$  could have changed the apparent relationship between the processes forming the biogenic sediment and the climatic factors driving those processes.

It is notable that sardine SDR is does not correlate with any geochemical proxies, because anchovy and hake show correlations with geochemical proxies, and because anchovy, hake, and sardine SDRs are all positively correlated. Thus, the presence of an in-phase or anti-phase pattern of anchovy and sardine abundance hypothesized by previous literature may not be controlled by the environmental conditions represented by the geochemical proxies used in this study.

However, this lack of correlation does support the conclusion of a 2012 study in which sardine biomass in Southern California was found to have no significant correlation with fluctuations in the PDO over a period of 370 years (McClatchie, 2012). For the years 1000-1500 CE of SPR0901-02KC (the same core used in this study), no correlation was found between sardine SDR and PDO, Pacific SST anomalies, and upwelling diatoms (Skrivanek and Hendy, 2015). This suggests that sardine SDRs in this core are consistent when they do not appear to respond to reconstructed environmental parameters over long timescales.

## Conclusions

Studying long-term changes in pelagic fish populations can provide a deeper understanding of how these fish interact with their environment that can then be used to predict responses to commercial fishing as well as anthropogenic climate change. This study focused on anchovy, sardine, hake, and surfperch populations in Santa Barbara Basin (SBB) off the coast of Southern California from 510 to 1910 CE. Fish scale counts from well-dated core SPR0901-02KC were used to generate absolute abundance, scale deposition rates (SDRs), and relative abundance (%) of each species. With the exception of a few ~100-year intervals, the absolute abundances of anchovy, sardine, and hake (SDRs) were all found to fluctuate in phase with one another. This finding contradicts the popular hypothesis that anchovy and sardine populations fluctuate in alternating regimes that are characterized by opposing environmental conditions (Chavez et al., 2003; Salvatteci et al., 2018). This does support conclusions drawn by several other studies, however, which state that anchovy and sardine populations generally fluctuate in phase over periods of >100 years and hypothesize their out-of-phase fluctuation to be an anomaly caused by commercial fishing (Field et al., 2009; McCall et al., 2009; Finney et al., 2010; McClatchie, 2012; McClatchie et al., 2017).

Both anchovy and hake SDRs correlated with periods of drought (low Ti content of the sediment). As drought and coastal upwelling are both caused by a strong NPH, this indicates that these species flourish during periods of coastal upwelling (Hendy et al., 2015), supporting the hypothesis that anchovy fare best in upwelling conditions (Chavez et al., 2003; Valdés et al., 2008; McClatchie et al., 2017; Salvatteci et al., 2018). However, this study found no correlation between anchovy abundance and the phytoplankton species that are believed to be associated with coastal upwelling (Abrantes and Moita, 1997; Anderson et al., 2008; Venrick ,1998), and

periods of sardine dominance over other species were found to be associated with increased carbon export. If carbon export is directly related to high marine biomass, then this result disagrees with the hypothesis that sardine dominate during periods of relatively low biological productivity (Chavez et al., 2003; Valdés et al., 2008; Salvatteci et al., 2018). Hake abundance was found to be potentially associated with poleward flow caused by a strong CU, which supports similar findings by Agostini et al. (2006).

These results suggest that the anchovy-sardine regime model may be too simplistic to accurately predict how fish populations interact with environmental changes such as coastal upwelling in the future. As current commercial fishing policies are based on these models, this improved understanding of forage fish population response to environmental change could make the industry more sustainable, further protecting these species and the industry from future collapse. As these species are an integral part of the coastal marine food web, collapse of forage fish populations will have a deleterious impact on higher-level consumers and primary producers.

Fig. 1. Collection location map of Kasten cores SPR0901-02KC, SPR0901-03KC, SPR0901-06KC, and ODP 893 in the Santa Barbara Basin (SBB) off the coast of Southern California, USA. Black arrows indicate surface ocean currents. Bathymetry and topography are shown in 100 m increments.

Fig. 2. Light microscope images of scales of studied species from SPR0901-02KC: A) Northern anchovy (*Engraulis mordax*), B) Pacific sardine (*Sardinops sagax*), C) Surfperch (Embiotocidae spp.), D) Hake (*Merluccius productus*). Scale bar = 1mm.

Fig. 3. Scale deposition rates (number  $\times 1000 \text{ cm}^{-2} \text{ yr}^{-1}$ ) of A) Northern anchovy, B) Pacific sardine, C) hake, and D) surfperch. Lines indicate total counted scales (whole scales plus fragments); shaded bars indicate counted whole (unbroken) scales.

Fig. 4. A) Ratio of sardine to anchovy scales on a logarithmic scale. Ratio of total scales is represented by black lines; ratio of whole scales is represented by red squares. B) Relative abundance (%) of total anchovy (dark blue), sardine (light blue), hake (green), and surfperch (yellow) scales. C) Scale deposition rates (number  $\times 1000 \text{ cm}^{-2} \text{ yr}^{-1}$ ) of total anchovy scales (blue line) and total sardine scales (red line). D) Scale deposition rates (number  $\times 1000 \text{ cm}^{-2} \text{ yr}^{-1}$ ) of total hake scales (green line) and total surfperch scales (purple line).

Fig. 5. Comparison of Northern anchovy, Pacific sardine, hake, and surfperch total scale deposition rates to geochemical data from nearby SPR0901-03KC. A)  $\delta^{15}\text{N}$  (‰), a proxy for coastal upwelling (Wang et al, in prep). B) Scanning XRF Ca/Ti (navy line), an indicator of biogenic  $\text{CaCO}_3$  production, and Si/Ti (red line), an indicator of biogenic  $\text{SiO}_2$  production (Hendy et al., 2015). C) Scanning XRF Ti (counts per second  $\times 10^3$ , black line), a proxy for sedimentation rates of lithogenic material deposited by river runoff, and Br/Cl (purple line), a proxy for total organic carbon and biogenic sedimentation rates (Hendy et al., 2015). D) Scale deposition rates (number  $\times 1000 \text{ cm}^{-2} \text{ yr}^{-1}$ ) of total anchovy scales (blue line) and total sardine scales (red line). E) Scale deposition rates (number  $\times 1000 \text{ cm}^{-2} \text{ yr}^{-1}$ ) of total hake scales (green line) and total surfperch scales (purple line). All data was resampled at a 5-year timestep.

Fig. 6 and 7. Average scale deposition rates of Kasten cores SPR0901-02KC and SPR0901-06KC for A) Northern anchovy (blue circles), B) Pacific sardine (red circles), C) hake (green circles), and D) surfperch (purple circles). Lightest shades represent whole scale SDRs, medium shades represent scale fragment SDRs, and darkest shades represent total scale SDRs. Bars represent 1 standard deviation. Time frames of 775-810, 945-1065, and 1675-1900 CE were chosen for core comparison based on known periods of extreme drought, when SDRs are expected to be particularly high.

Table 1. Original and corrected (for instantaneous depositional events) depths of marker horizons in SPR0901-02KC with the corresponding calibrated calendar age (Du et al., 2018).

Assigned Age (years C.E.)	Marker Horizon Type	Uncorrected Depth Top of Horizon	Uncorrected Depth Bottom of Horizon	Depth cm BCT corrected
1910	Core top	0	0.0	2
1860	Grey flood layer	13.0	13.9	13.00
1840	Olive turbidite layer	16.6	-	15.70
1810	Olive turbidite layer	24.0	-	23.10
1761	Grey flood layer	32.5	34.4	31.60
1737	Olive turbidite layer	38.4	44.8	35.60
1685	Marker Laminae #1A	50.9	-	41.70
1643	Marker Laminae #1B	57.0	-	47.80
1574	Marker Laminae #2	64.8	-	55.50
1530	Grey flood layer	69.4	73.9	60.10
1463	Marker Laminae #3	79.3	-	65.50
1380	Grey flood layer	87.5	88.0	73.70
1263	Grey flood layer	98.5	101.0	84.10
1193	Marker Laminae #4	109.1	-	92.40
1095	Olive turbidite layer	115.5	120.4	98.80
1022	Marker Laminae #5	126.7	-	105.10
952	Marker Laminae #6	132.6	-	111.00
855	Marker Laminae #7	139.7	-	118.10
763	Grey flood layer	146.6	147.4	125.00
676	Olive turbidite layer	153.0	157.4	130.60
641	Grey flood layer	160.0	163.4	133.20
516	Marker Laminae #8	172.5	-	142.30
440	Grey flood layer	177.4	178.5	147.20
338	Marker Laminae #9	185.1	-	153.80
272	Grey flood layer	190.4	190.5	159.10
200	Olive turbidite layer	197.8	202.4	166.30
112	Marker Laminae #10	212.8	-	176.80
64	Grey flood layer	218.2	231.0	182.20
27	Olive turbidite layer	235.4	241.5	186.60
-15	Marker Laminae #11	248.7	-	193.80
-87	Grey flood layer	253.7	256.3	198.80
-155	Grey flood layer	259.6	260.2	202.10
-184	Grey flood layer	263.4	264.5	205.30
-205	Grey flood layer	266.5	267.8	207.30
-215	Grey flood layer	269.7	271.0	207.90

Table 2. Pearson correlation coefficients between scale deposition rates (SDRs) and relative abundance (%) of anchovy, sardine, hake, and surfperch as well as sardine to anchovy scale ratio (total scales). n = 281.

Sardine SDR	Hake SDR	Surf-perch SDR	Anchovy %	Sardine %	Hake %	Surf-perch %	Sardine/Anchovy ratio	
0.329	0.409	0.086	0.491	-0.256	-0.238	-0.268	-0.288	Anchovy SDR
	0.111	0.192	-0.132	0.530	-0.214	-0.007	0.426	Sardine SDR
		-0.083	-0.22	-0.309	0.608	-0.309	-0.211	Hake SDR
			-0.190	0.067	-0.193	0.732	0.236	Surfperch SDR
				-0.417	-0.633	-0.391	-0.482	% Anchovy
					-0.308	0.175	0.686	% Sardine
						-0.175	-0.103	% Hake
							0.343	% Surfperch

Table 3. Pearson correlation coefficient for scale deposition rates (SDRs) and relative abundance (%) of all four fish species, sardine to anchovy scale ratio (total scales),  $\delta^{15}\text{N}$  (denitrified source water proxy; Wang et al, in prep), Br/Cl (carbon export proxy; Wang et al, in prep), Ca/Ti (biogenic  $\text{CaCO}_3$  proxy; Wang et al, in prep), Ti (lithogenic sedimentation proxy; Du et al., in prep), and Si/Ti (biogenic  $\text{SiO}_2$  proxy; Hendy et al., 2015). Positive to negative correlation shown as a gradient from orange to blue. n = 281.

$\delta^{15}\text{N}$	Br/Cl	Ca/Ti	Ti	Si/Ti	
0.186	-0.227	0.213	-0.210	0.140	Anchovy SDR
0.040	0.033	0.117	-0.095	0.022	Sardine SDR
0.223	-0.261	0.047	-0.274	0.061	Hake SDR
-0.093	0.027	0.095	0.056	-0.139	Surfperch SDR
0.025	-0.050	0.056	0.085	0.176	% Anchovy
-0.112	0.253	0.005	0.031	-0.084	% Sardine
0.158	-0.166	-0.033	-0.197	-0.051	% Hake
-0.224	0.097	-0.067	0.164	-0.177	% Surfperch
-0.115	0.243	-0.012	-0.007	-0.087	Sardine/Anchovy ratio
	-0.165	0.490	-0.287	0.239	$\delta^{15}\text{N}$
		0.107	0.109	0.292	Br/Cl
			-0.368	0.207	Ca/Ti
				-0.286	Ti

## References

- Abrantes, F., Moita, M.T., 1999. Water column and recent sediment data on diatoms and coccolithophorids, off Portugal, confirm sediment record of upwelling events. *Oceanologica Acta* 22, 67–84.
- Agostini, V.N., Francis, R.C., Hollowed, A.B., Pierce, S.D., Wilson, C., Hendrix, A.N., 2006. The relationship between Pacific hake (*Merluccius productus*) distribution and poleward subsurface flow in the California Current System. *Canadian Journal of Fisheries and Aquatic Sciences* 63, 2658–2659. doi:[10.1139/F06-139](https://doi.org/10.1139/F06-139)
- Alverson, D.L., Larkins, H.A., 1969. Status of knowledge of the Pacific Hake resource. *California Cooperative Oceanic Fisheries Investigations Reports* 13, 24–31.
- Anderson, C.R., Siegel, D.A., Brzezinski, M.A., Guillocheau, N., 2008. Controls on temporal patterns in phytoplankton community structure in the Santa Barbara Channel, California. *Journal of Geophysical Research* 113, C04038. doi:[10.1029/2007JC004321](https://doi.org/10.1029/2007JC004321)
- Barron, J.A., Burky, D., Hendy, I.L., 2015. High-resolution paleoclimatology of the Santa Barbara Basin during the Medieval Climate Anomaly and early Little Ice Age based on diatom and silicoflagellate assemblages in Kasten core SPR0901-02KC. *Quaternary International* 387, 13–22. doi:[10.1016/j.quaint.2014.04.020](https://doi.org/10.1016/j.quaint.2014.04.020)
- Baumgartner, T.R., Soutar, A., Ferreira-Bartrina, V., 1992. Reconstruction of the history of Pacific sardine and northern anchovy populations over the past two millennia from sediments of the Santa Barbara Basin, California. *California Cooperative Oceanic Fisheries Investigations Reports* 33, 24–40.
- Blaauw, M., Christen, J.A., 2011. Flexible paleoclimate age-depth models using an autoregressive gamma process. *Bayesian Analysis* 6, 457–474.
- Brzezinski, M.A., Washburn, L., 2011. Phytoplankton primary productivity in the Santa Barbara Channel: Effects of wind-driven upwelling and mesoscale eddies. *Journal of Geophysical Research* 116, C12013. doi:[10.1029/2011JC007397](https://doi.org/10.1029/2011JC007397)
- Chavez, F.P., Ryan, J., Lluch-Cota, S.E., 2003. From anchovies to sardines and back: multidecadal change in the Pacific Ocean. *Science* 299, 217–221.
- Chavez, E.A., Chavez-Hidalgo, A., 2013. The sardine fishery of the Gulf of California. *California Cooperative Oceanic Fisheries Investigations Reports* 54, 205–214.
- Checkley Jr., D.M., Barth, J.A., 2009. Patterns and processes in the California Current System. *Progress in Oceanography* 83, 49–64. doi:[10.1016/j.pocean.2009.07.028](https://doi.org/10.1016/j.pocean.2009.07.028)
- Checkley Jr., D.M., Dotson, R.C., Griffith, D.A., 2000. Continuous, underway sampling of eggs of Pacific sardine (*Sardinops sagax*) and northern anchovy (*Engraulis mordax*) in spring 1996 and 1997 off southern and central California. *Deep Sea Research II* 47, 1139–1155.
- Checkley Jr., D.M., Asch, R.G., Rykaczewski, R.R., 2017. Climate, Anchovy, and Sardine. *Annual Review of Marine Science* 9, 469–493. doi:[10.1146/annurev-marine-122414-033819](https://doi.org/10.1146/annurev-marine-122414-033819)
- Contreras-Reyes, J.E., Canales, T.M., Rojas, P.M., 2016. Influence of climate variability on anchovy reproductive timing off northern Chile. *Journal of Marine Systems* 164, 67–75. doi:[10.1016/j.jmarsys.2016.08.006](https://doi.org/10.1016/j.jmarsys.2016.08.006)
- Cubillos, L.A., Arcos, D.F., 2002. Recruitment of common sardine (*Strangomerina bentincki*) and anchovy (*Engraulis ringens*) off central-south Chile in the 1990s and the impact of the 1997–1998 El Niño. *Aquatic Living Resources* 15, 87–94.

- Demer, D.A., Zwolinski, J.P., Byers, K.A., Cutter, G.R., Renfree, J.S., Sessions, T.S., Macewicz, B.J., 2012. Prediction and confirmation of seasonal migration of Pacific sardine (*Sardinops sagax*) in the California Current Ecosystem. *Fishery Bulletin* 110, 52–70.
- Du, X., Hendy, I., Schimmelmann, A., 2018. A 9000-year flood history for Southern California: A revised stratigraphy of varved sediments in Santa Barbara Basin. *Marine Geology* 397, 29–42. doi:[10.1016/j.margeo.2017.11.014](https://doi.org/10.1016/j.margeo.2017.11.014)
- Du, X., Hendy, I.L., Wang, Y., in prep. The relationship between annual precipitation variability and ENSO in Southern California for the Common Era (last 2,000 years). *Nature Geoscience*.
- Field, D.B., Baumgartner, T.R., Ferreira, V., Gutiérrez, D., Lozano-Montes, H., Salvatteci, R., Soutar, A., 2009. Chapter 4. Variability from scales in marine sediments and other historical records. In: Checkley Jr., D.M., Alheit, J., Oozeki, Y. (Eds.), *Climate Change and Small Pelagic Fish*. Cambridge University Press, New York.
- Finney, B.P., Alheit, J., Emeis, K.-C., Field, D.B., Gutiérrez, D., Struck, U., 2010. Paleoecological studies on variability in marine fish populations: A long-term perspective on the impacts of climatic change on marine ecosystems. *Journal of Marine Systems* 79, 316–326. doi:[10.1016/j.jmarsys.2008.12.010](https://doi.org/10.1016/j.jmarsys.2008.12.010)
- Hamman, M.G., Nevarez-Martínez, M.O., Green-Ruis, Y., 1998. Spawning habitat of the pacific sardine (*Sardinops sagax*) in the Gulf of California: egg and larval distribution 1956-1957 and 1971-1991. *California Cooperative Oceanic Fisheries Investigations Reports* 39, 169–179.
- Hendy, I.L., Dunn, L., Schimmelmann, A., 2013. Resolving varve and radiocarbon chronology differences during the last 2000 years in the Santa Barbara Basin sedimentary record, California. *Quaternary International* 310, 155–168. doi:[10.1016/j.quaint.2012.09.006](https://doi.org/10.1016/j.quaint.2012.09.006)
- Hendy, I.L., Napier, T.J., Schimmelmann, A., 2015. From extreme rainfall to drought: 250 years of annually resolved sediment deposition in Santa Barbara Basin, California. *Quaternary International* 387, 3–12. doi:[10.1016/j.quaint.2015.01.026](https://doi.org/10.1016/j.quaint.2015.01.026)
- Heusser, L.E., Hendy, I.L., Barron, J.A., 2015. Vegetation response to southern California drought during the Medieval Climate Anomaly and early Little Ice Age (AD 800-1600). *Quaternary International* 387, 23–35. doi:[10.1016/j.quaint.2014.09.032](https://doi.org/10.1016/j.quaint.2014.09.032)
- Jacobson, L.D., MacCall, A.D., 1995. Stock recruitment models for Pacific sardine (*Sardinops sagax*). *Canadian Journal of Fisheries and Aquatic Sciences* 52, 566–577.
- Koslow, J.A., Goericke, R., Watson, W., 2013. Fish assemblages in the Southern California Current: relationships with climate, 1951–2008. *Fisheries Oceanography* 22, 207–219. doi:[10.1111/fog.12018](https://doi.org/10.1111/fog.12018)
- Kuwae, M., Yamamoto, M., Sagawa, T., Ikehara, K., Irino, T., Takemura, K., Takeoka, H., Sugimoto, T., 2017. Multidecadal, centennial, and millennial variability in sardine and anchovy abundances in the western North Pacific and climate–fish linkages during the late Holocene. *Progress in Oceanography* 159, 86–98. doi:[10.1016/j.pocean.2017.09.011](https://doi.org/10.1016/j.pocean.2017.09.011)
- Kucas Jr., S.T., Parsons, J., 1986. Species profiles: life histories and environmental requirements of coastal fishes and Invertebrates (Pacific Southwest)--northern anchovy. U.S. Fish and Wildlife Service Biological Report 82.
- Lindgren, M., Checkley Jr., D.M., Rouyer, T., MacCall, A.D., Stenseth, N.C., 2013. Climate, fishing, and fluctuations of sardine and anchovy in the California Current. *Proceedings of the National Academy of Sciences of the United States of America* 110, 13672–13677.
- Lingen, C.D. van der, Bertrand, A., Bode, A., Brodeur, R., Cubillos, L.A., Espinoza, P., Friedland, K., Garrido, S., Irigoien, X., Miller, T., Möllmann, C., Rodriguez-Sanchez, R., Tanaka, H.,

- Temming, A., 2009. Chapter 7: Trophic dynamics. In: Checkley Jr., D.M., Alheit, J., Oozeki, Y. (Eds.), *Climate Change and Small Pelagic Fish*. Cambridge University Press, New York.
- Lynn, R.J., Simpson, J.J., 1987. The California Current System: the seasonal variability of its physical characteristics. *Journal of Geophysical Research* 92, 12.947-12.966.
- MacCall, A.D., 2009. Chapter 12. Mechanisms of low-frequency fluctuations in sardine and anchovy populations. In: Checkley Jr., D.M., Alheit, J., Oozeki, Y. (Eds.), *Climate Change and Small Pelagic Fish*. Cambridge University Press, New York.
- McCabe-Glynn, S., Johnson, K.R., Strong, C., Berkelhammer, M., Sinha, A., Cheng, H., Edwards, R.L., 2013. Variable North Pacific influence on drought in southwestern North America since AD 854. *Nature Geoscience* 6. doi:[10.1038/NGEO1862](https://doi.org/10.1038/NGEO1862)
- McClatchie, S., 2012. Sardine biomass is poorly correlated with the Pacific Decadal Oscillation off California. *Geophysical Research Letters* 39. doi:[10.1029/2012GL052140](https://doi.org/10.1029/2012GL052140)
- McClatchie, S., Goericke, R., Hill, K., 2010. Re-assessment of the stock–recruit and temperature–recruit relationships for Pacific sardine (*Sardinops sagax*). *Journal of Fisheries and Aquatic Sciences* 67, 1782–1790. doi:[10.1139/F10-101](https://doi.org/10.1139/F10-101)
- McClatchie, S., Hendy, I.L., Thompson, A.R., Watson, W., 2017. Collapse and recovery of forage fish populations prior to commercial exploitation. *Geophysical Research Letters* 44. doi:[10.1002/2016GL071751](https://doi.org/10.1002/2016GL071751)
- McClatchie, S., Vetter, R.D., Hendy, I.L., 2018. Forage fish, small pelagic fisheries and recovering predators: managing expectations. *Animal Conservation*. doi:[10.1111/acv.12421](https://doi.org/10.1111/acv.12421)
- Napier, T.J., Hendy, I.L., Hinnov, L.A., Brown, E.T., Shevenell, A., 2018. Subtropical hydroclimate during Termination V (~430–422 ka): Annual records of extreme precipitation, drought, and interannual variability from Santa Barbara Basin 191, 73–88.
- Patterson, T.R., Wright, C., Chang, A.S., Taylor, L.A., Lyons, P.D., Dallimore, A., Kumar, A., 2002. Atlas of common squamatological (fish scale) material in coastal British Columbia and an assessment of the utility of various scale types in paleofisheries reconstruction. *Palaeontologia Electronica* 4.
- Rykaczewski, R.R., Checkley Jr., D.M., 2008. Influence of ocean winds on the pelagic ecosystem in upwelling regions. *Proceedings of the National Academy of Sciences of the United States of America* 105, 1965–1970. doi:[10.1073/pnas.0711777105](https://doi.org/10.1073/pnas.0711777105)
- Salvatteci, R., Field, D., Gutiérrez, D., Baumgartner, T.R., Ferreira, V., Ortlieb, L., Sifeddine, A., Grados, D., Bertrand, A., 2018. Multifarious anchovy and sardine regimes in the Humboldt Current System during the last 150 years. *Global Change Biology*. doi:[10.1111/gcb.13991](https://doi.org/10.1111/gcb.13991)
- Schimmelmann, A., Lange, C.B., Berger, W.H., Simon, A., Burke, S.K., Dunbar, R.B., 1992. Extreme climatic conditions recorded in Santa Barbara Basin laminated sediments: the 1835–1840 Macoma event. *Marine Geology* 106, 279–299.
- Schroeder, I.D., Black, B.A., Sydeman, W.J., Bograd, S.J., Hazen, E.L., Santora, J.A., Wells, B.K., 2013. The North Pacific High and wintertime pre-conditioning of California current productivity. *Geophysical Research Letters* 40, 1–6. doi:[10.1002/grl.50100](https://doi.org/10.1002/grl.50100)
- Schwartzlose, R.A., Alheit, J., Bakun, A., Baumgartner, T.R., Cloete, R., Crawford, R.J.M., Fletcher, W.J., Green-Ruis, Y., Hagen, E., Kawaski, T., Lluch-Belda, D., Lluch-Cota, S.E., MacCall, A.D., Matsuura, Y., Nevarez-Martínez, M.O., Parrish, R.H., Roy, C., Serra, R., Shust, K.V., Ward, M.N., Zuzunaga, J.Z., 1999. Worldwide large-scale fluctuations of sardine and anchovy populations. *South African Journal of Marine Science* 21, 289–349.

- Skrivanek, A., Hendy, I.L., 2015. A 500 year climate catch: Pelagic fish scales and paleoproductivity in the Santa Barbara Basin from the Medieval Climate Anomaly to the Little Ice Age (AD 1000–1500). *Quaternary International* 36–45. doi:[10.1016/j.quaint.2015.07.044](https://doi.org/10.1016/j.quaint.2015.07.044)
- Soutar, A., Isaacs, J.D., 1974. Abundance of pelagic fish during the 19th and 20th centuries as recorded in anaerobic sediment off the Californias. *Fishery Bulletin* 72, 257–273.
- Valdés, J., Ortlieb, L., Gutiérrez, D., Marinovic, L., Vargas, G., Sifeddine, A., 2008. 250 years of sardine and anchovy scale deposition record in Mejillones Bay, northern Chile. *Progress in Oceanography* 79, 198–207.
- Venrick, E.L., 1998. The phytoplankton of the Santa Barbara Basin: patterns of chlorophyll and species structure and their relationships with those of surrounding stations. *California Cooperative Oceanic Fisheries Investigations Reports* 39.
- Wang, Y., Hendy, I.L., Napier, T.J., 2017. Climate and anthropogenic controls of coastal deoxygenation on interannual to centennial timescales. *Geophysical Research Letters* 44, 11528–11536. doi:[10.1002/2017GL075443](https://doi.org/10.1002/2017GL075443)
- Wang, Y., Hendy, I.L., Du, X., in prep. The relationship between ocean circulation and marine productivity in Northeast Pacific for the last two thousand years. *Paleoceanography*.
- Winant, C.D., Dorman, C.E., 1997. Seasonal patterns of surface wind stress and heat flux over the Southern California Bight. *Journal of Geophysical Research* 102, 5641–5653.
- Zhao, M., Eglinton, G., Read, G., Schimmelmann, A., 2000. An alkenone ( $\text{U}37\kappa'$ ) quasi-annual sea surface temperature 37 record (A.D. 1440 to 1940) using varved sediments from the Santa Barbara Basin. *Organic Geochemistry* 31, 903–917. doi:[10.1016/S0146-6380\(00\)00034-6](https://doi.org/10.1016/S0146-6380(00)00034-6)

**Figure 1**

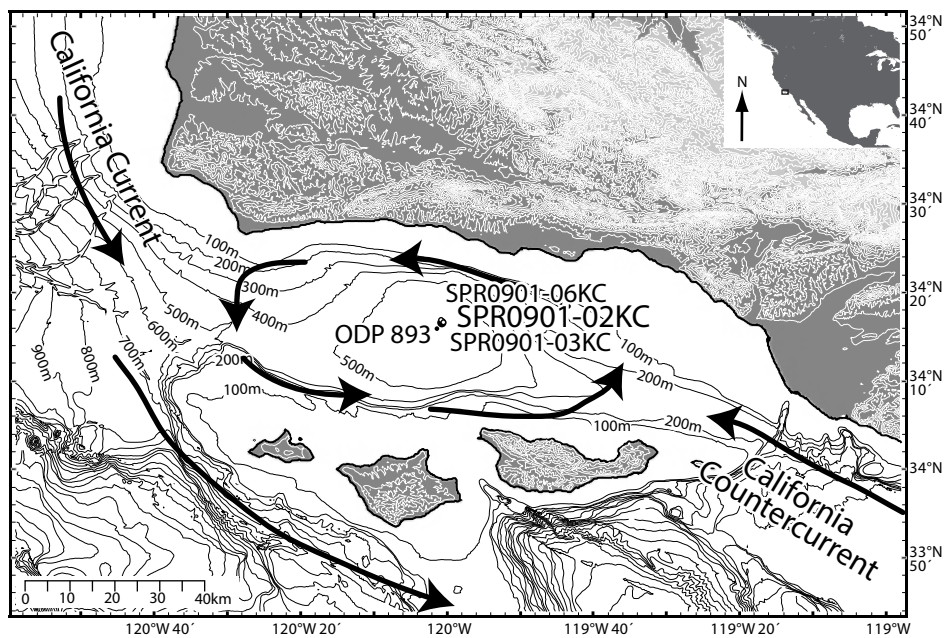


Figure 2

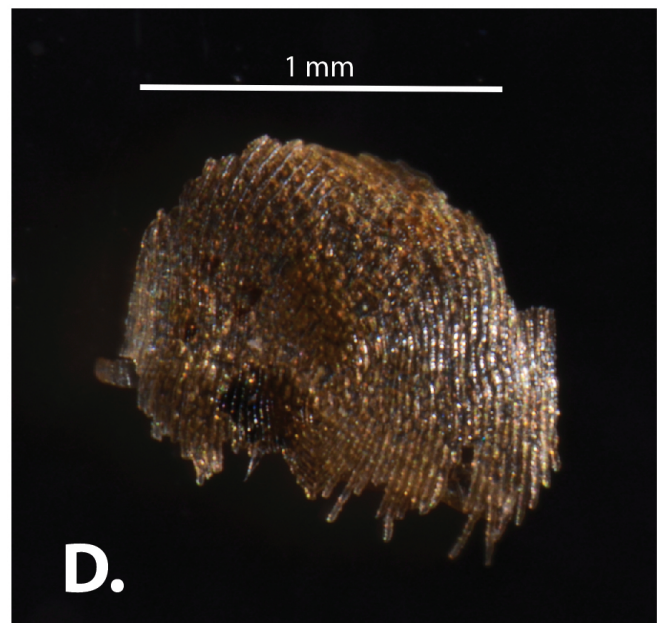
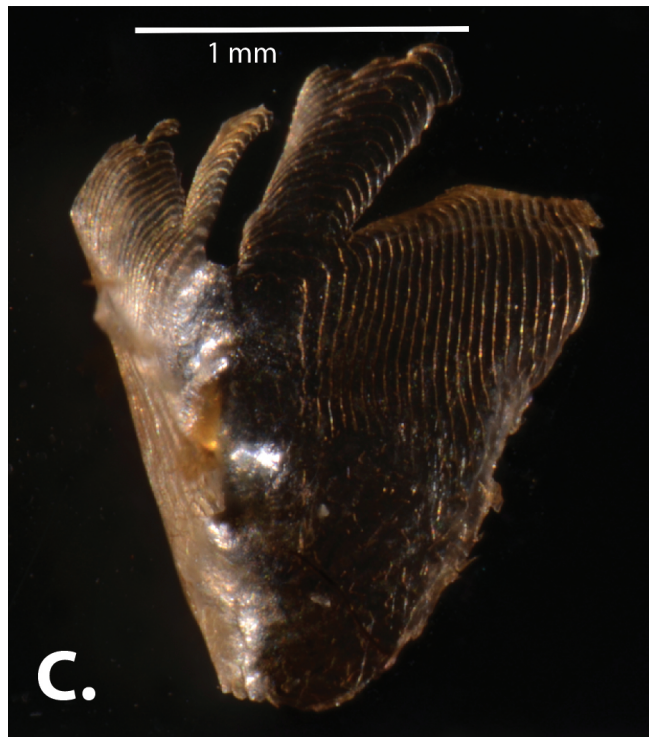
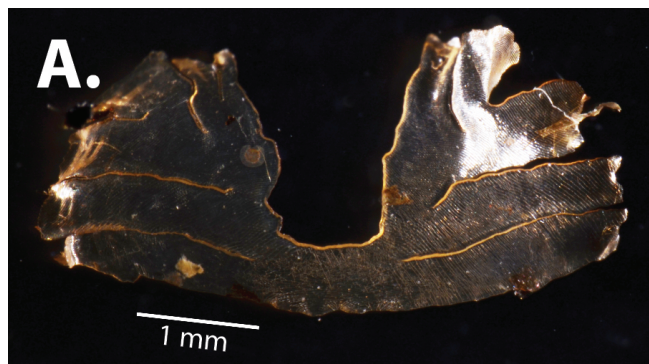


Figure 3

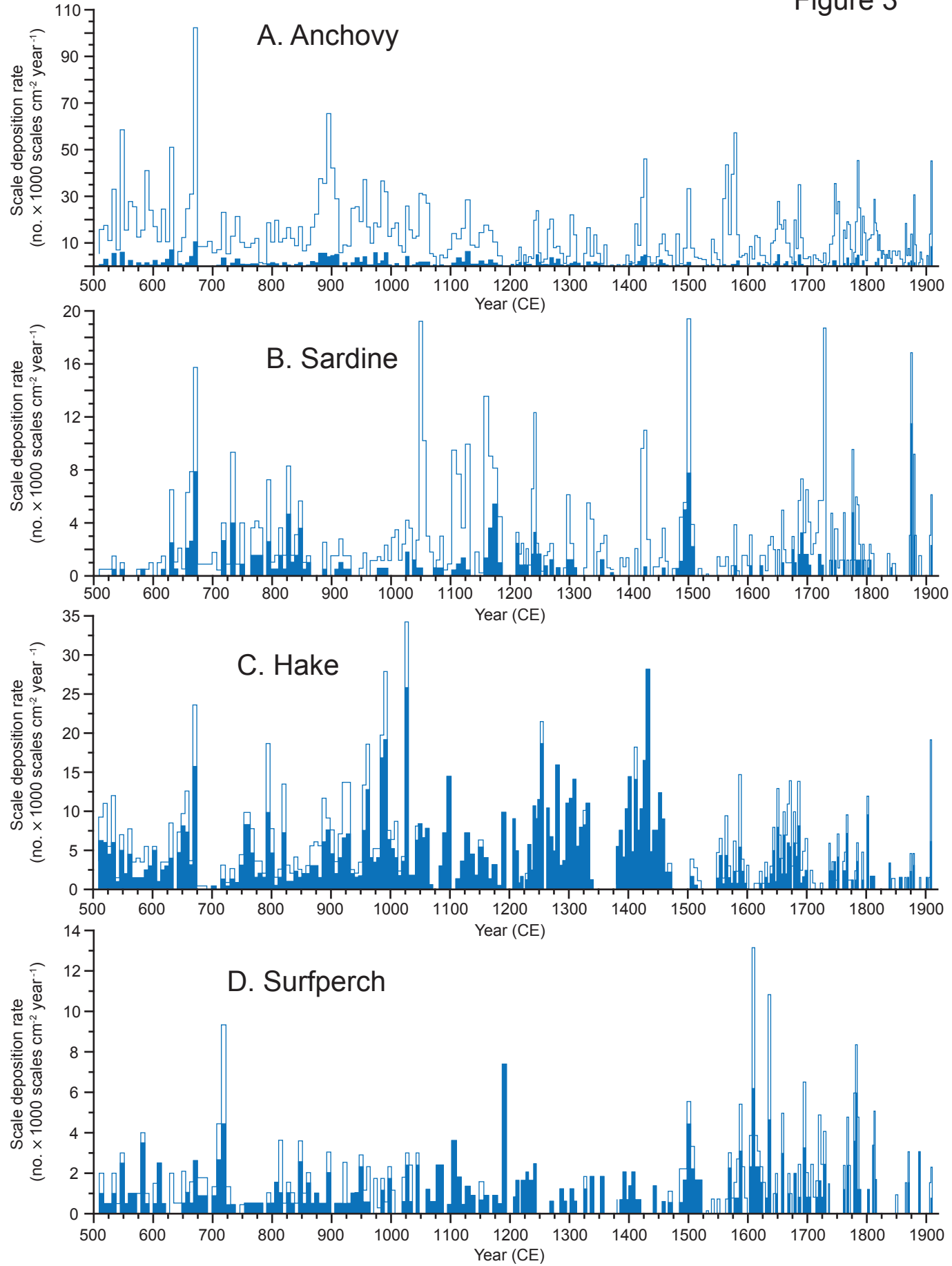


Figure 4

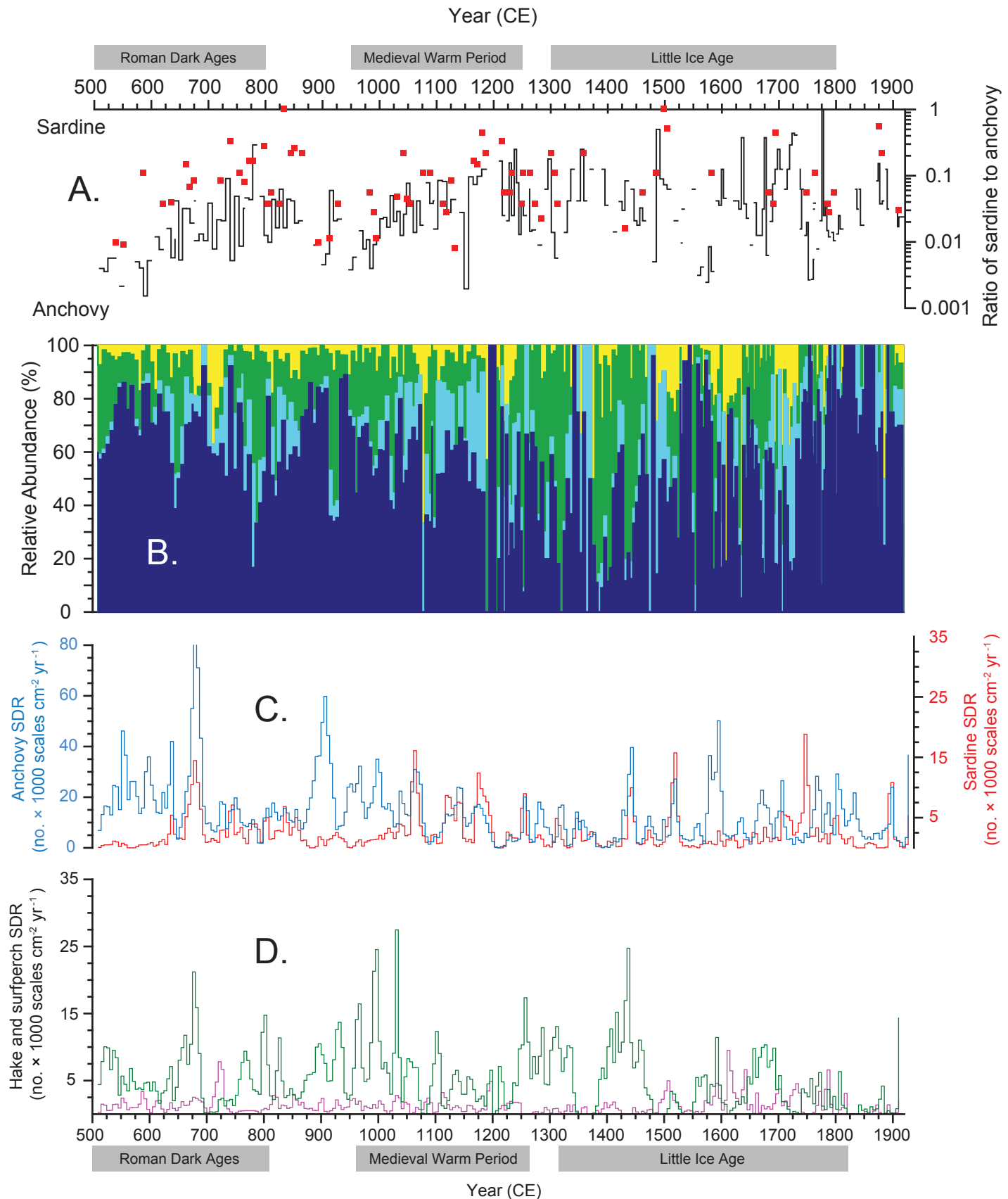


Figure 5

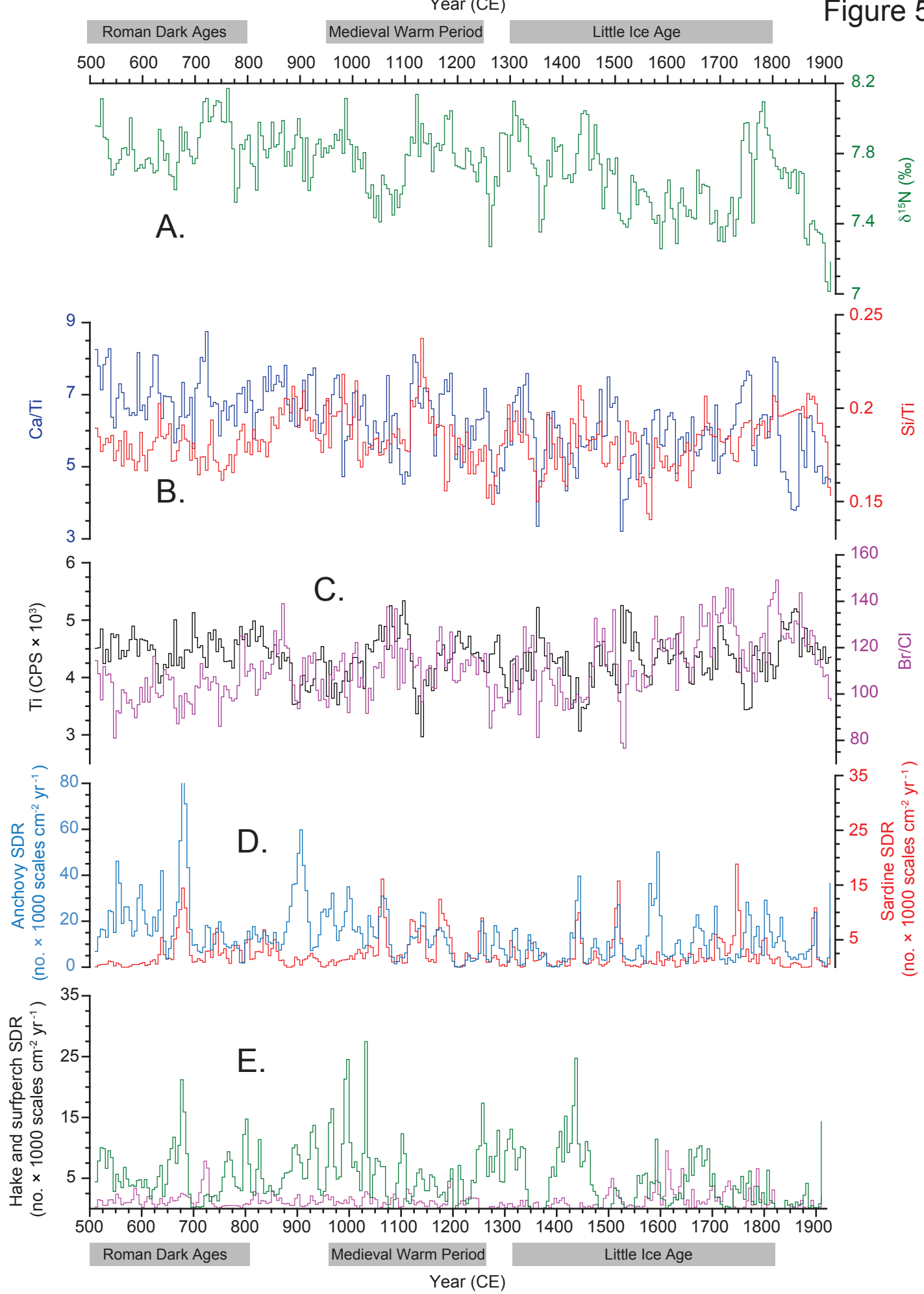


Figure 6

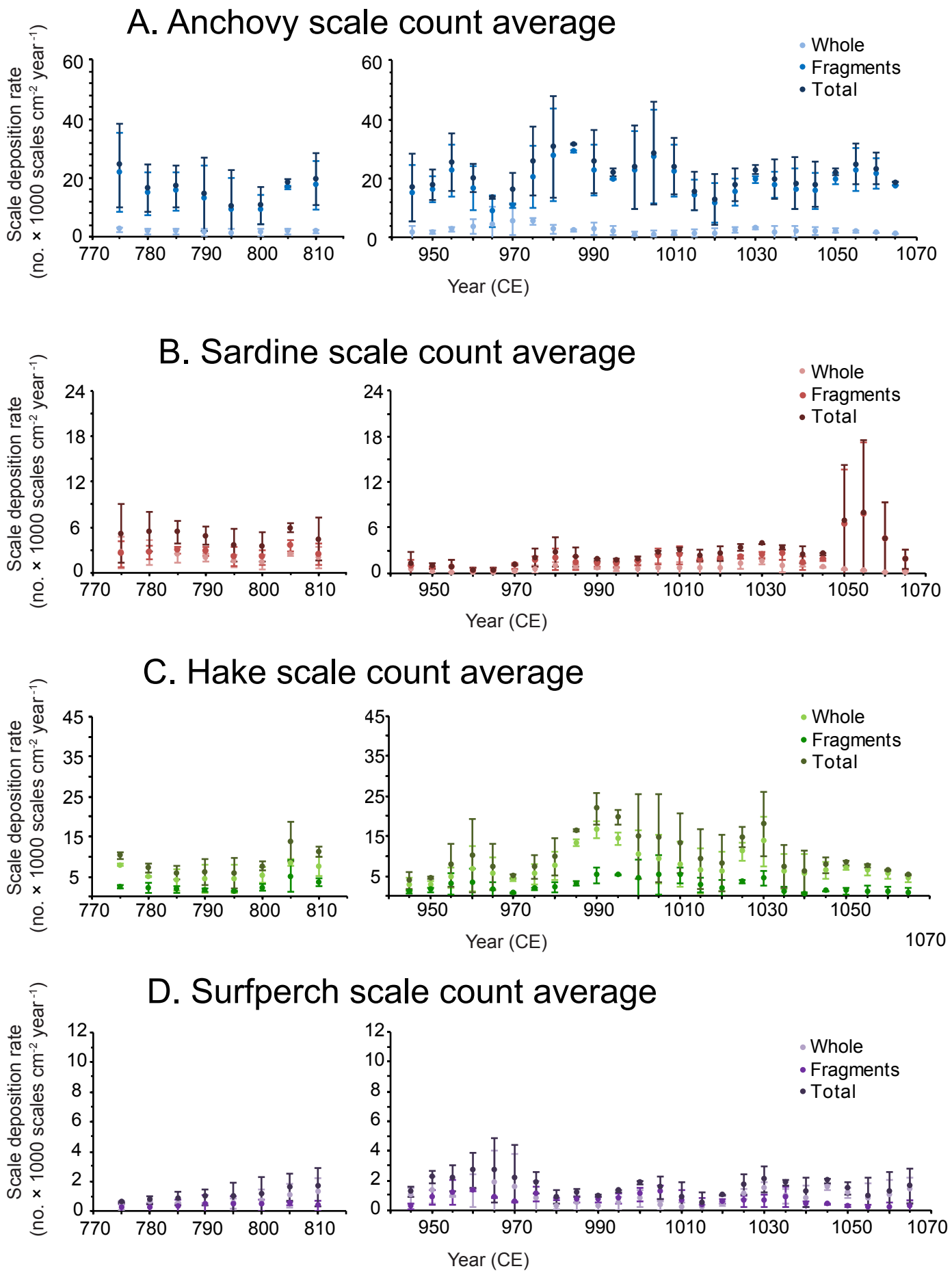


Figure 7

